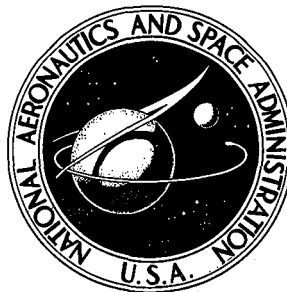


NASA TECHNICAL NOTE



NASA TN D-4923

NASA TN D-4923

THE EFFECTS OF REACTOR RADIATION ON 22-VOLT SILICON VOLTAGE-REGULATOR DIODES

by Suzanne T. Weinstein

Lewis Research Center

Cleveland, Ohio

THE EFFECTS OF REACTOR RADIATION ON 22-VOLT
SILICON VOLTAGE-REGULATOR DIODES

By Suzanne T. Weinstein

Lewis Research Center
Cleveland, Ohio

NATIONAL AERONAUTICS AND SPACE ADMINISTRATION

For sale by the Clearinghouse for Federal Scientific and Technical Information
Springfield, Virginia 22151 - CFSTI price \$3.00

ABSTRACT

Twenty-five silicon voltage-regulator (Zener) diodes (S1N2985B) were exposed to reactor radiation to a total fast-neutron fluence of 8.2×10^{13} neutrons per square centimeter and a gamma dose of 6.3×10^7 rads carbon. The Zener voltage remained essentially constant and the breakdown knee was somewhat softened. The forward and reverse-leakage currents increased, and the forward voltage drop at high forward currents increased. The junction capacitance remained unchanged.

THE EFFECTS OF REACTOR RADIATION ON 22-VOLT SILICON VOLTAGE-REGULATOR DIODES

by Suzanne T. Weinstein

Lewis Research Center

SUMMARY

Twenty-five silicon voltage-regulator (Zener) diodes (S1N2985B) were exposed to reactor radiation at the NASA Plum Brook Reactor Facility. This 10-watt, 22-volt Zener diode was selected for radiation testing on the basis of its applicability to nuclear space-power-generation systems. This test is part of a series designed to provide design data for a variety of semiconductor components for such systems and to correlate radiation damage to the devices tested with current theories of damage mechanisms.

The diodes were exposed to a fast-neutron fluence of approximately 8.2×10^{13} neutrons per square centimeter and a gamma dose of approximately 6.3×10^7 rads carbon. The diodes were divided into three groups that were irradiated under different electrical operating conditions. The current-voltage characteristics of all diodes were measured before and after irradiation. In addition, junction capacitance at zero bias was determined for each diode before and after irradiation. The variation of capacitance with applied bias were measured on a few selected devices before irradiation.

The degradation of diode electrical characteristics was in agreement with theoretical damage predictions and with results reported previously on other Zener diodes. The Zener voltage remained essentially constant and the breakdown knee was somewhat softened. Forward- and reverse-leakage current increased due to a decrease in the minority carrier lifetimes, and the voltage drop at high forward currents increased. The junction capacitance remained unchanged.

INTRODUCTION

For some long-duration space missions, nuclear-generated electric systems are attractive when compared with other power systems such as batteries, fuel cells, or solar cells, especially where relatively large amounts of power are required. However,

nuclear electric power generating systems in space present a severe nuclear-radiation environment for the system components. Power conditioning and control are necessarily an integral part of a power system. Although semiconductor devices are desirable for this power conditioning and control because of their low weight, low power consumption, and high reliability, they are the most radiation-sensitive electrical components. Because of this radiation sensitivity, a shield weight may be more than what would be required for the power system if radiation-tolerant components were used. It is desirable therefore to define more exactly the radiation tolerance of presently available semiconductor power devices that would be used in space-power systems.

A testing program was developed to investigate the effects of reactor radiation on such semiconductor devices (ref. 1). In the work described herein, a 22-volt silicon voltage-regulator (Zener) diode was tested in a reactor; the experiment was designed primarily to provide data for system design. Correlation of diode behavior with present day theories of device operation was also attempted.

Work performed by others (see ref. 2) indicates that voltage-regulator diodes are the least radiation-sensitive semiconductor components. However, the diodes previously tested have lower power ratings and, therefore, smaller junction areas than the S1N2985 diodes. Junction area, in some semiconductor devices, appears to have a significant effect on radiation tolerance.

EXPERIMENT DESIGN AND PROCEDURES

Diode Description

The silicon voltage-regulator diode selected for this test was the S1N2985B, which is a 22-volt (± 5 percent), 10-watt silicon Zener diode that maintains voltage regulation by avalanche breakdown. The prefix S indicates that these diodes meet a screening specification for semiconductor devices established by the NASA Marshall Space Flight Center (ref. 3). This specification includes visual and radiographic examination, acceleration, shock and vibration testing, high-temperature bake, thermal cycling, and a power burn-in. The electrical characteristics of S1N2985B are presented in table I. The diode junction is circular with a diameter of approximately 2 millimeters. The overall thickness of the silicon chip is 0.23 millimeter (maximum) and the base is p-type. The diodes are mounted in welded, hermetically sealed metal and glass cases with the stud being the anode.

TABLE I. - ELECTRICAL CHARACTERISTICS OF S1N2985B AT 25° C

Zener voltage at test current, V_Z , V	
Minimum	20.9
Nominal	22.0
Maximum	23.1
Zener impedance at test current, Z_{ZT} , ohm	5.0
Zener test current, I_{ZT} , mA	115
Zener impedance at 1 mA, Z_{ZK} , ohm	250
Voltage regulation ^a , V_Z , V	1.4
Reverse leakage at 18.8 V, I_{R1} , μ A	3.0
Reverse leakage at 18.8 V and 50° C, I_{R2} , μ A	10
Maximum Zener direct current, I_{ZM} , A	0.43
Maximum Zener surge current, I_{ZS} , A	2.18

^aDifference in Zener voltage at 0.2 and 0.04 A.

Diode Irradiation

Twenty-five S1N2985B diodes, drawn from a single lot, were irradiated in the HB-6 beam port of the NASA Plum Brook Reactor Facility.) The diodes were mounted on a circular, water-cooled, aluminum plate, 38.1 centimeters in diameter and 0.635 centimeter thick, which was positioned perpendicular to the reactor beam. The stud temperature of each diode was monitored by a Chromel-Alumel thermocouple. Figure 1 shows the installation of a diode on the test plate (fig. 1(a)) and the arrangement of the diodes on the plate with the corresponding diode code numbers (fig. 1(b)). The remainder of the plate was occupied by a group of twenty-five 4.7-volt silicon voltage-regulator diodes.

The diodes were irradiated for four reactor cycles, (numbers 50 P to 53 P) each consisting nominally of 10 days at a reactor power level of 60 megawatts. The average total fast-neutron fluence (above 0.1 MeV) for the four cycles was 8.2×10^{13} neutrons per square centimeter, ± 35 percent, and the average gamma dose was 6.3×10^7 rads carbon, ± 20 percent. These dose levels are at least a factor of 10 larger than the estimated dose level for a space-power-system mission lasting 1 year. The average fast neutron fluence and average gamma-ray dose are defined for the center of the HB-6 beam port center (see fig. 1) and a reactor power level of 60 megawatts. References 5 to 7 provide discussions of the neutron and gamma-ray flux mapping of the HB-6 facility.

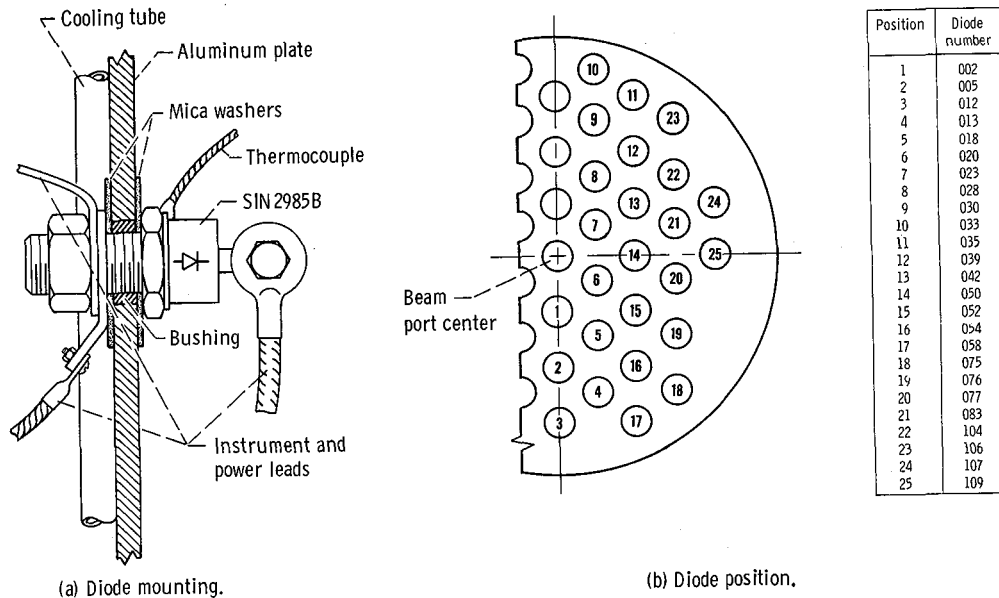


Figure 1. - Irradiation assembly.

TABLE II. - DIODE OPERATING CONDITIONS DURING IRRADIATION^a

Plate position	Group	Operating conditions
1 to 15	A	200 mA; dc bias at 50 percent maximum Zener current
16 to 20	B	11 V; dc bias at 50 percent nominal Zener voltage
21 to 25	C	200±100 mA; modulated dc at 50±25 percent maximum Zener current

^aSee fig. 1 for diode number-plate position correlation.

The diodes were electrically energized during irradiation. In order to determine the effects of electrical operation on radiation damage, the devices were divided into three different operating modes, as shown in table II. During irradiation, the case temperature of the diodes in groups A and C was approximately 65^o C, and that of group B was approximately 50^o C.

Preirradiation and Postirradiation Testing

The current-voltage characteristics and the junction capacitance at zero applied bias were measured on each diode before and after irradiation. In addition, the variation

of junction capacitance with applied bias was determined for a few diodes. All measurements were made at room temperature (27° C). Characteristic curves were plotted and the data were analyzed in terms of present-day p-n junction theory.

Reverse characteristics. - The reverse-leakage current was measured at 19 pre-selected voltage points from 5.0 millivolts to 20.0 volts. The Zener voltage was measured at 13 current points from 0.1 to 400 milliamperes.

Forward characteristics. - The forward current was determined at 13 voltage points from 5.0 to 500 millivolts. The forward voltage drop was measured at 17 current points from 0.1 milliamperes to 5.0 amperes.

Junction capacitance. - Junction capacitance was measured at an alternating current signal of 0.02 volt peak-to-peak at 10 kilohertz. The variation of capacitance with applied direct-current bias was measured at 13 forward voltage points from 50.0 to 300 millivolts and reverse voltage points from 0.05 to 15.0 volts. These measurements were made on diodes 1, 7, 16, and 21.

ANALYSIS AND DISCUSSION

There are two basic neutron-irradiation damage mechanisms that affect the characteristics of semiconductor devices. Electrically active defects are introduced that result in a decrease in the net carrier concentration. Recombination levels within the energy band gap are also introduced causing decreased minority carrier lifetimes.

Effects of Carrier Removal

Neutron irradiation introduces electrically active defects in silicon, which cause a decrease in the net carrier concentration. This carrier removal will eventually produce heavily compensated, intrinsic material at high neutron doses. Stein (ref. 8) has determined carrier removal rates in silicon under fission spectrum neutron irradiation. The removal rates vary from 3 to 10 carriers per neutron-centimeter. The removal rate remains nearly constant for low initial carrier concentrations but rises sharply for concentrations above 10^{15} carriers per cubic centimeter. There is also a slight dependence of the removal rate on the crystal growth process and the dopant type.

Junction Capacitance

The junction capacitance was measured to estimate the diode doping levels and profile and to determine the effects of radiation on these properties.

Junction capacitance as a function of applied reverse bias was measured on a few selected diodes. Figure 2 is a plot of $1/C^3$ as a function of applied bias for one diode; the resulting straight line indicates that the linearly-graded assumption may be valid. (Symbols are defined in the appendix.) The grade constant was calculated from the slope of this curve using equation (1) for the capacitance of a linearly graded junction (ref. 9).

$$C = A \left[\frac{q\epsilon^2 a}{12(V_B - V_A)} \right]^{1/3} \quad (1)$$

where q is the electron charge, ϵ is the dielectric permittivity, A is the junction area, a is the grade constant, V_B is the built-in potential, and V_A is the applied voltage. The calculated grade constant is 3.9×10^{21} centimeters⁻⁴. At $1/C^3 = 0$, the intercept (0.45 V) should be the built-in voltage; however, Muss (ref. 10) and others have shown that this extrapolation will not give the true built-in voltage. But it can be obtained from the grade constant and the depletion region width W_0 at zero bias (ref. 9).

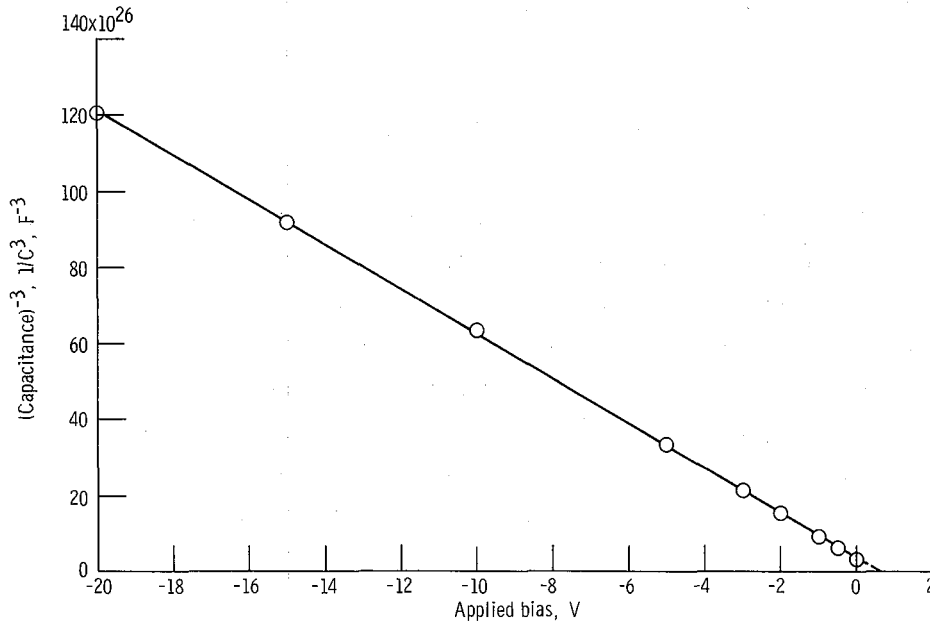


Figure 2. - Capacitance⁻³ as function of voltage for diode 7.

$$V_B = \frac{kT}{q} \ln \left(\frac{aW_o}{2n_i} \right)^2 \quad (2)$$

where n_i is the intrinsic carrier density and W_o is given by

$$W_o = \frac{\epsilon A}{C_o} = 2.1 \times 10^{-5} \text{ cm} \quad (3)$$

where C_o is the zero bias capacitance. The calculated built-in voltage is 0.77 volt.

The base region doping level can also be calculated from the above data, with the assumption that the junction is linearly graded (see ref. 9):

$$N_B = \frac{aW_o}{2} = 3.8 \times 10^{16} \text{ cm}^{-3} \quad (4)$$

The junction capacitance of these diodes was not significantly affected by radiation damage at the fast neutron fluence of 8.2×10^{13} neutrons per square centimeter. When a conservative carrier removal rate of 10 carriers per neutron per centimeter is assumed, the removal carrier density for this irradiation is 8×10^{14} carriers per cubic centimeter which is approximately 2 percent of the calculated base doping density. The corresponding 2-percent decrease in the grade constant would cause a decrease in the junction capacitance of about 0.7 percent. Changes of this size in the zero-bias capacitance were observed. However, variations of this size may also be the result of experimental error.

Voltage Regulation Region

The reference, or Zener, voltage of silicon voltage regulator diodes is insensitive to radiation damage at moderate dose levels. The reference voltage of this type of diode is maintained by avalanche multiplication; that is, carriers acquire sufficient energy in the junction field to produce additional electron-hole pairs by impact ionization. The breakdown voltage at which carrier multiplication becomes infinite is a function of the grade constant a for a diffused, linearly graded junction. This breakdown voltage in silicon (ref. 11) is given by

$$V_{br} = 1.71 \times 10^9 a^{-0.364} \quad (5)$$

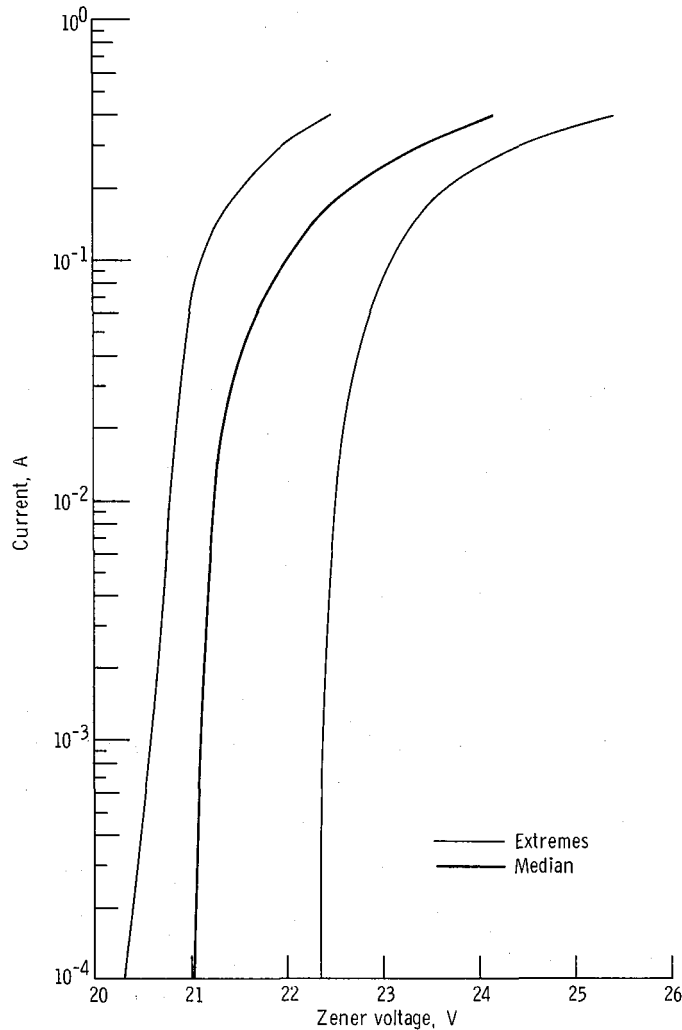


Figure 3. - Zener voltage as function of current for median and extremes (pre- and postirradiation indistinguishable).

The 2-percent decrease in the grade constant, due to carrier removal at the neutron fluence of 8.2×10^{13} neutrons per square centimeter, should produce an increase in the reference voltage of about 0.7 percent. The measured change in the reference voltage at 200 milliamperes (approximately 50 percent maximum current) was less than 0.6 percent in all cases. Figure 3 shows a plot of the reference voltage as a function of current for the median and the extremes. The preirradiation and postirradiation cases are indistinguishable. The breakdown knee was somewhat softened in all but three diodes, which showed a slight hardening. It was not possible to identify the radiation damage mechanism that caused knee softening.

The neutron failure dose for these diodes can be estimated, if diode failure is defined as a 20-percent increase in the nominal Zener voltage. For a conservative carrier removal rate of 10 carriers per neutron per centimeter, the failure dose for these diodes is approximately 1×10^{15} neutrons per square centimeter. Work performed by others (ref. 2) has shown that radiation-induced changes in the Zener voltage appear at neutron doses of 10^{15} to 10^{16} neutrons per square centimeter. It appears that increased junction area does not affect the radiation tolerance of the Zener voltage.

High Forward Current Region

The forward current at high applied voltages (greater than the built-in voltage) becomes limited by space charge and other effects. Jonscher (ref. 12) has derived a relation for space-charge limited current flow:

$$I^{1/2} = \left(\frac{q^2 \mu N_B A}{8kT d} \right)^{1/2} (V_A - V_B) \quad (6)$$

where μ is the base minority carrier mobility and d is the width of the base region. The current-voltage characteristics of all diodes exhibited this behavior before and after irradiation. Figure 4 is a plot of the square root of the current as a function of the applied voltage minus the built-in voltage before and after irradiation for the median and extremes. The decrease in slope due to radiation is too large to be accounted for by

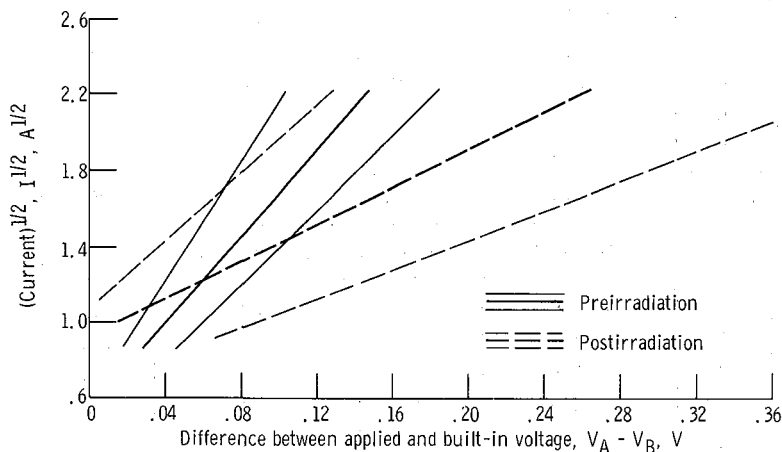


Figure 4. - Square root of forward current as function of difference between applied and built-in voltage before and after irradiation for median and extremes.

TABLE III. - CHANGE IN FORWARD VOLTAGE DROP AND
PREIRRADIATION FORWARD DROP AT 1.0 AND 5.0

Diode	Current, I, A			
	1.0		5.0	
	Preirradiation voltage drop, V	Change, V	Preirradiation voltage drop, V	Change, V
Group A; Zener current, 200 mA				
1	0.813	-0.010	0.929	0.117
2	.800	.001	.879	.141
3	.808	.012	.905	.202
4	.809	.043	.914	.269
5	.809	.020	.926	.221
6	.798	.107	.878	.157
7	.810	-.013	.917	.133
8	.807	-.040	.917	.009
9	.820	-.022	.939	.091
10	.818	-.032	.926	.037
11	.797	-.030	.871	.155
12	.830	-.030	.958	.086
13	.822	.014	.945	.135
14	.802	.006	.897	.115
15	.809	-.023	.925	.105
rms	-----	0.036	-----	0.146
Group B; reverse voltage, 11 V				
16	0.794	-0.030	0.876	0.024
17	.815	.011	.942	.123
18	.811	.028	.906	.045
19	.795	.031	.876	.022
20	.807	.040	.907	.011
rms	-----	0.030	-----	0.060
Group C; Zener current, 200±100 mA				
21	0.816	-0.018	0.945	0.110
22	.807	.043	.913	-.002
23	.816	.041	.926	.016
24	.812	.044	.924	-.004
25	.816	.049	.919	-.006
rms	-----	0.040	-----	0.045

carrier removal. The mobility change required to account for these slope decreases is much larger than the mobility changes reported by Stein (ref. 8). It appears that the slope as given in equation (6) is not appropriate to these diodes.

Table III lists the change in forward voltage drop and the preirradiation forward voltage drop at 1.0 and 5.0 amperes for all diodes. The operating mode during irradiation appears to affect the forward voltage drop, particularly at higher currents as can be noted in table III at 5.0 amperes. This dependence on operating mode was also noticed in the average decreases in slope of 53, 38, and 28 percent for groups A, B, and C, respectively.

Effects of Decreased Carrier Lifetime

Neutron irradiation introduces recombination levels in the band gap which results in decreased carrier lifetimes. These decreased lifetimes produce increases in the reverse bias leakage current and in the low forward currents at forward biases below the built-in voltage.

The reverse-leakage current and the low forward current (at biases up to 400 mV for these diodes) in silicon are recombination-generation currents. The current is given by (ref. 13)

$$I = \frac{qn_i WA}{\sqrt{\tau_{n_o} \tau_{p_o}}} \frac{2 \sinh\left(\frac{qV_a}{2kT}\right)}{\frac{q(V_B - V_A)}{kT}} f(b) \quad (7)$$

where τ_{n_o} and τ_{p_o} are the minority carrier lifetimes in p- and n-type material, respectively, and

$$b = e^{-qV_A/2kT} \cosh\left[\frac{(E_T - E_i)}{kT} + 2 \ln\left(\frac{\tau_{p_o}}{\tau_{n_o}}\right)\right] \quad (8)$$

where $E_T - E_i$ is the difference between the trap level and the center of the band gap; then for $b < 1.0$

$$f(b) = \frac{1}{(1 - b^2)^{1/2}} \left\{ \frac{\pi}{2} \tan^{-1} \left[\frac{b}{(1 - b^2)^{1/2}} \right] \right\} \quad (9)$$

and for $b > 1.0$

$$f(b) = \frac{1}{2(b^2 - 1)^{1/2}} \ln \left[\frac{b + (b^2 - 1)^{1/2}}{b - (b^2 - 1)^{1/2}} \right] \quad (10)$$

At forward biases above about 400 millivolts, there is a significant contribution to the forward current due to diffusion current, which becomes dominant as the applied bias approaches the built-in potential. The diffusion current is given by (ref. 9)

$$I = \frac{qD_n n_p A}{L_n} \left(e^{qV_A/kT} - 1 \right) = \frac{q \sqrt{D_n} n_i^2 A}{N_B \sqrt{\tau_{n_0}}} \left(e^{qV_A/kT} - 1 \right) \quad (11)$$

where n_p is the electron concentration in the base, D_n is the electron diffusion constant, and L_n is the electron diffusion length.

Calculation of the slopes of $\ln I$ versus V in various regions indicated that equations (8) and (12) describe these diodes. Values of the carrier lifetimes and effective trap level were calculated from the forward characteristics of the diodes by applying these equations at three voltage points as follows:

The base minority carrier lifetime τ_{n_0} was calculated at 700 millivolts using equation (12). Equation (8) was applied at 100 and 250 millivolts where recombination-generation current dominates. At 250 millivolts, b was assumed to be small so that $f(b)$ is approximately $\pi/2$, and the hole lifetime τ_{p_0} was calculated. These lifetimes were then used at 100 millivolts to obtain a value of $f(b)$, and then b was taken from a curve. The trap level was then calculated from

$$\frac{E_T - E_i}{kT} = \pm \cosh^{-1} \left(b e^{qV_A/2kT} \right) - \frac{1}{2} \ln \left(\frac{\tau_{p_0}}{\tau_{n_0}} \right) \quad (12)$$

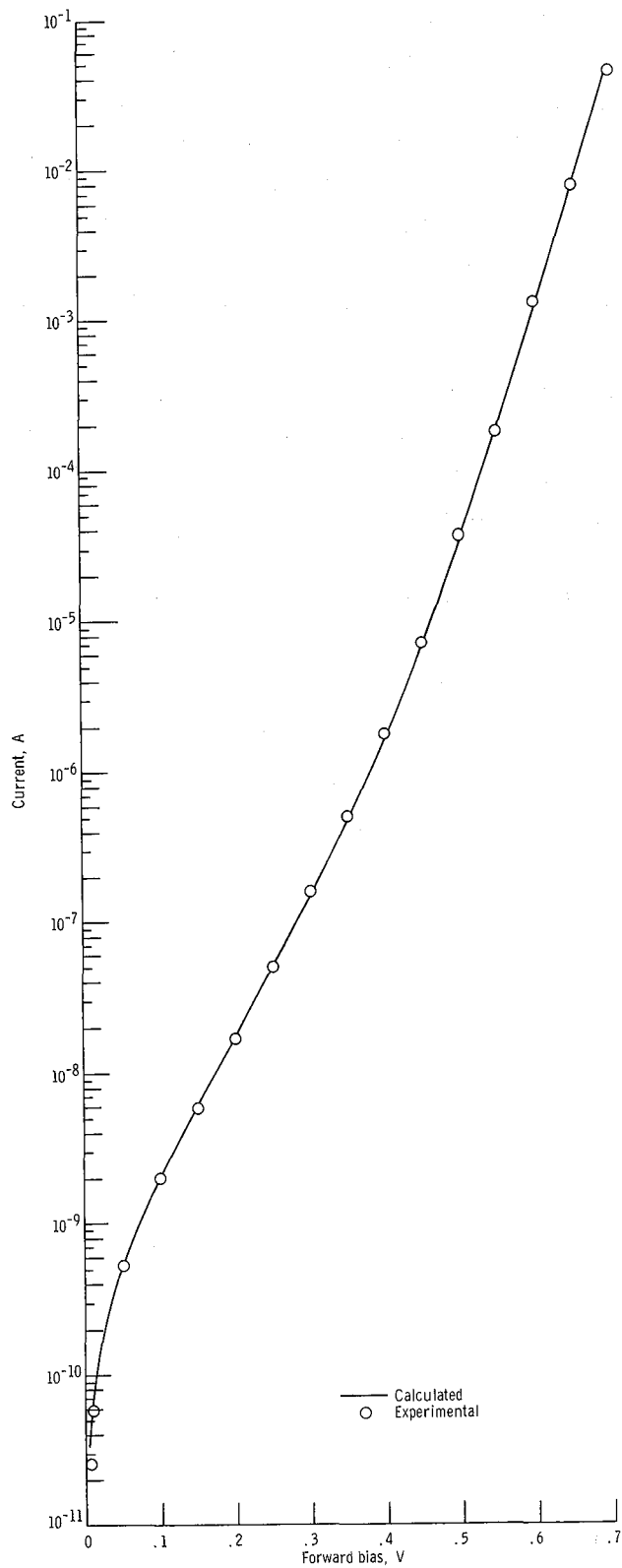


Figure 5. - Comparison of experimental and calculated forward characteristics for diode 1 (typical).

These calculations were made for each diode before and after irradiation, and the values were used to generate the forward and reverse characteristics. Figures 5 and 6 are plots of the calculated curves with the experimental points indicated for a typical diode (1) before irradiation. The agreement of calculated with experimental values below 1.0 volt in the reverse direction indicates that the calculated lifetimes are realistic. The deviation above 1.0-volt reverse bias in figure 6 is due to the onset of carrier multiplication, which is not a function of minority carrier lifetime. In all other regions, the agreement of calculated and experimental values was good for all diodes before and after irradiation.

Table IV presents the calculated carrier lifetimes and the square root of their product before and after irradiation. As can be seen in the table, the mean electron lifetime (25 diodes) decreased by a factor of 37. The mean hole lifetime decreased by a factor of 3. The mean effective lifetime, defined as $\sqrt{\tau_{n_0} \tau_{p_0}}$ decreased by a factor of 10.

At reverse biases greater than several kT/q , equation (7) can be approximated as (ref. 13)

$$I = \frac{qn_i W A}{2 \sqrt{\tau_{n_0} \tau_{p_0}}} \quad (13)$$

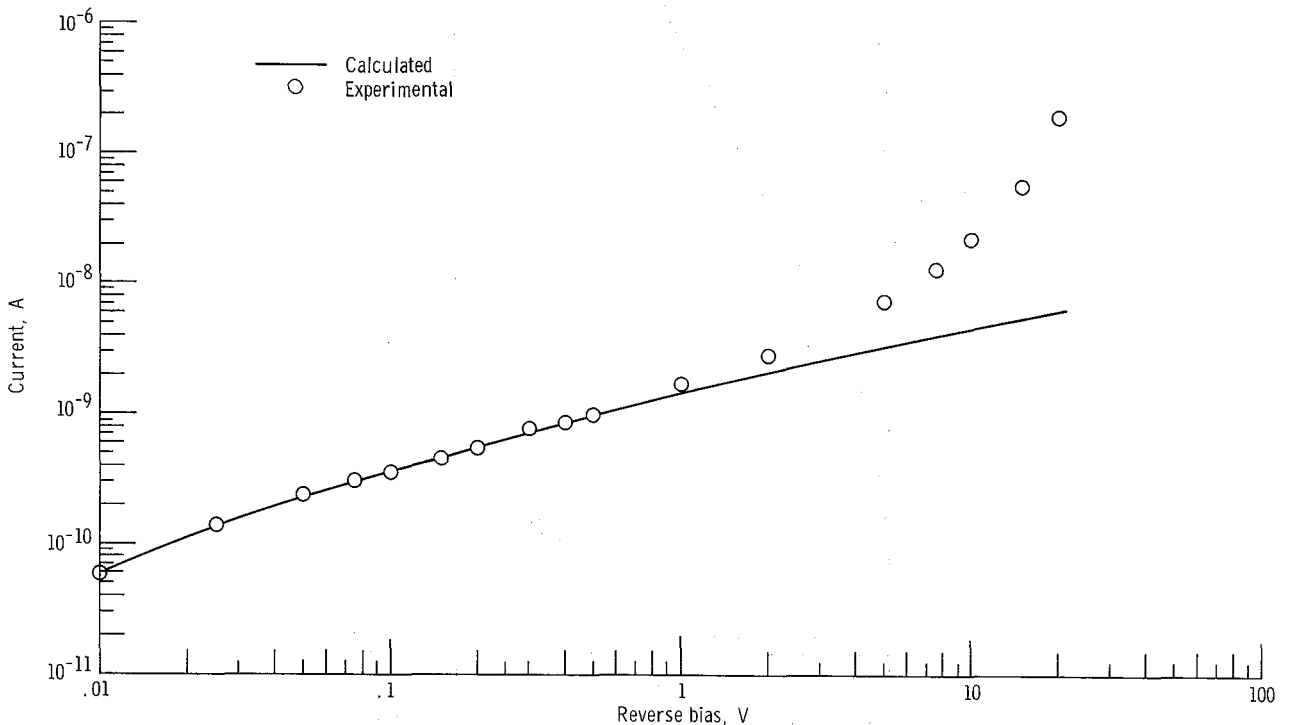


Figure 6. - Comparison of experimental and calculated reverse characteristics for diode 1 (typical).

TABLE IV. - MINORITY CARRIER LIFETIMES AND EFFECTIVE LIFETIME
BEFORE AND AFTER IRRADIATION AND DAMAGE CONSTANT

Diode	Preirradiation			Postirradiation			Damage constant, $K_T, [(nvt)(\text{sec})]^{-1}$
	Minority carrier lifetime, sec		Mean effective lifetime, $\sqrt{\tau_{p_0} \tau_{n_0}}$, sec	Minority carrier lifetime, sec		Mean effective lifetime, $\sqrt{\tau_{p_0} \tau_{n_0}}$, sec	
	In p-type material, τ_{n_0}' , sec	In n-type material, τ_{p_0}' , sec		In p-type material, τ_{n_0}' , sec	In n-type material, τ_{p_0}' , sec		
Group A; Zener current, 200 mA							
1	2.5×10^{-6}	2.3×10^{-8}	2.4×10^{-7}	6.7×10^{-8}	1.7×10^{-8}	3.3×10^{-8}	3.1×10^{-7}
2	2.5	1.7	2.1	5.1	.83	2.1	3.4
3	2.0	6.7	3.6	5.4	3.3	4.2	2.6
4	2.2	5.1	3.3	6.5	.61	2.0	5.9
5	2.2	7.3	4.0	8.0	2.3	4.2	2.6
6	.99	2.7	1.6	2.5	.81	1.4	7.8
7	1.8	.33	.77	5.7	.65	1.9	4.8
8	1.9	2.0	1.9	5.7	1.4	2.8	3.8
9	2.7	5.8	4.0	5.4	3.1	4.1	2.7
10	1.7	4.2	2.3	7.2	1.0	2.7	4.0
11	1.4	2.2	1.8	5.1	1.4	2.7	3.9
12	7.1	2.6	4.2	11.0	2.6	5.4	2.0
13	3.0	2.4	2.7	8.2	.55	2.3	4.4
14	1.2	20.0	4.9	3.7	1.9	2.6	4.4
15	1.9	8.0	3.9	6.5	2.0	3.6	3.1
Mean	2.3×10^{-6}	4.9×10^{-8}	2.9×10^{-7}	6.2×10^{-8}	1.6×10^{-8}	3.0×10^{-8}	3.9×10^{-7}
Group B; reverse voltage, 11 V							
16	1.2×10^{-6}	6.0×10^{-8}	2.7×10^{-7}	5.6×10^{-8}	0.59×10^{-8}	1.9×10^{-8}	6.3×10^{-7}
17	2.5	3.6	3.0	9.1	.59	2.8	4.9
18	2.9	5.5	4.0	7.3	.54	2.0	3.4
19	1.3	2.4	1.8	5.1	.59	1.7	6.4
20	2.3	4.8	3.3	5.1	.74	1.9	6.0
Mean	2.0×10^{-6}	4.5×10^{-8}	2.9×10^{-7}	6.4×10^{-8}	0.60×10^{-8}	2.1×10^{-8}	5.4×10^{-7}
Group C; Zener current, 200 mA \pm 100 mA							
21	3.0×10^{-6}	0.79×10^{-8}	1.5×10^{-7}	8.8×10^{-8}	1.7×10^{-8}	3.9×10^{-8}	2.4×10^{-7}
22	2.2	2.3	2.2	6.8	.70	2.2	5.1
23	4.7	5.3	5.0	8.6	1.6	3.7	3.0
24	2.7	4.3	3.5	7.2	2.0	3.7	2.9
25	3.5	4.4	3.9	6.5	1.3	2.7	3.9
Mean	3.2×10^{-6}	3.4×10^{-8}	3.2×10^{-7}	7.6×10^{-8}	1.5×10^{-8}	3.2×10^{-8}	3.5×10^{-7}

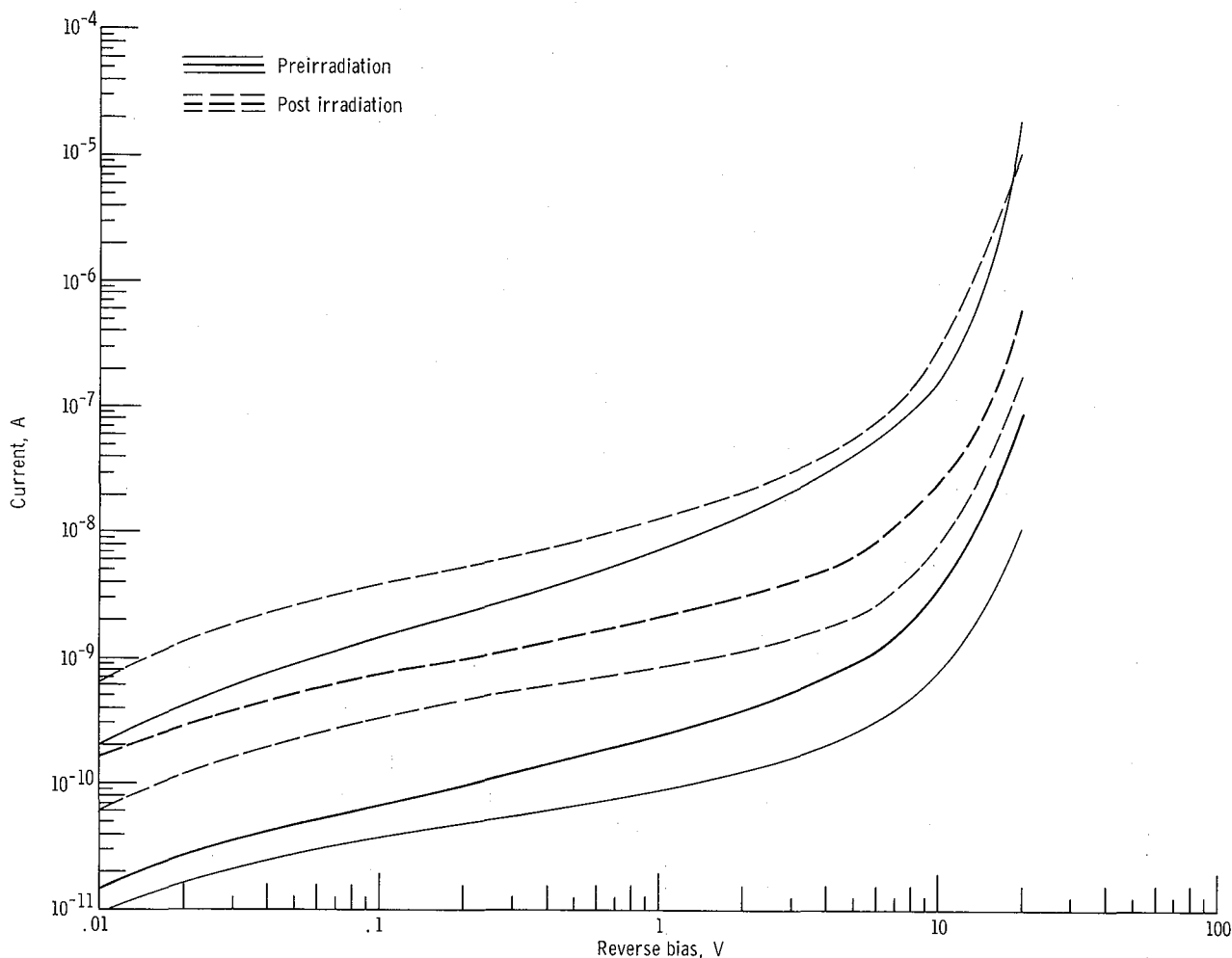


Figure 7. - Reverse leakage current as function of voltage before and after irradiation for median and extremes.

where W , the depletion region width, is the only voltage dependent factor. The effect of radiation damage can be determined from the effective lifetime which has been defined previously. The agreement of the observed changes in reverse-leakage current with changes in the effective lifetimes calculated for each diode was excellent for biases up to about 1 volt where carrier multiplication begins. The variation in leakage current among the diodes is considerable, but, in general, the lower the initial leakage, the larger the increase. Figure 7 is a plot of reverse leakage current as a function of applied bias for the median and the extremes before and after irradiation.

At low forward biases (below 400 mV), the equation for recombination-generation current (7) cannot be greatly simplified. The mean increase in forward current at these biases was approximately elevenfold. In this region, the increase in current is due to a decrease in the effective lifetime and also to an increase in $f(b)$. The lifetime decrease is the dominant effect, producing a factor of 10 increase in current. The remaining

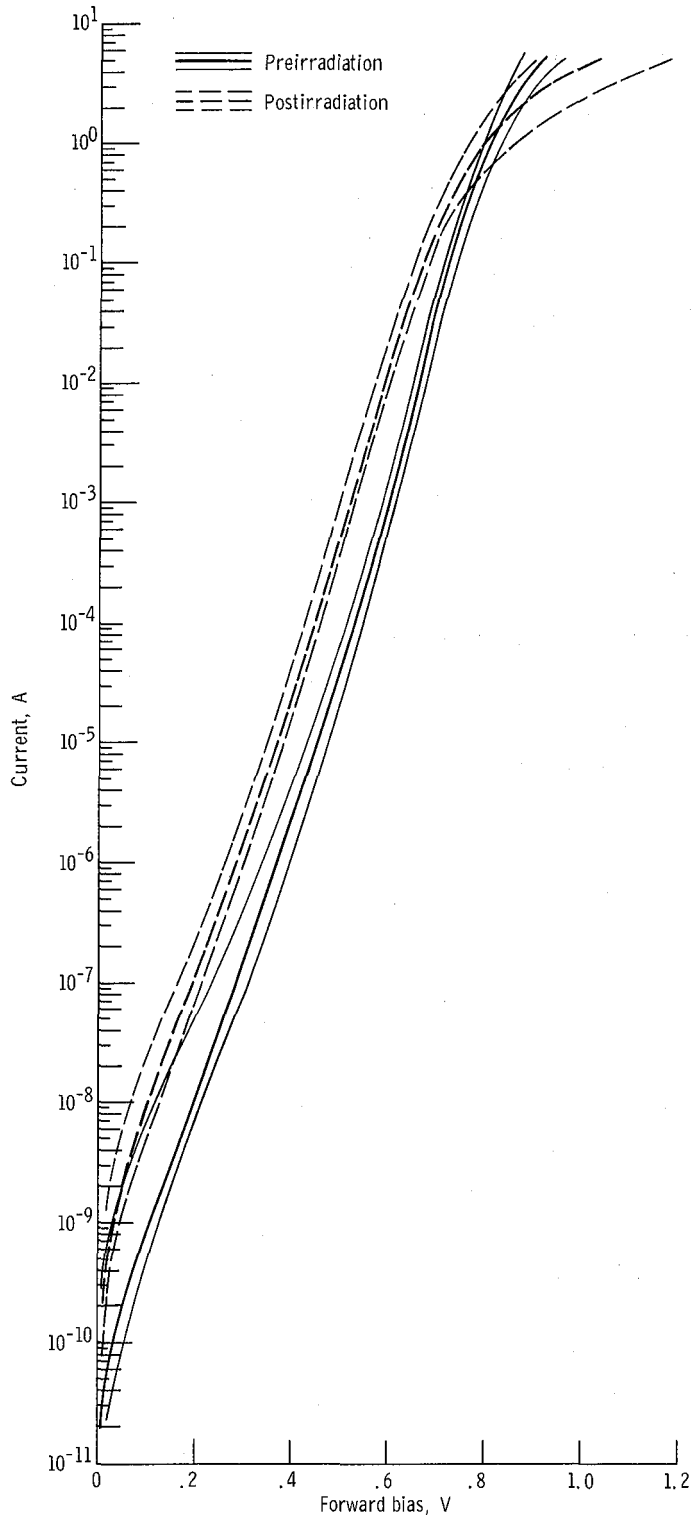


Figure 8. - Forward current as function of voltage before and after irradiation for median and extremes.

current increase can be accounted by the increase in $f(b)$, which is due primarily to the decrease in the ratio of the minority carrier lifetimes (eq. (8)). The trap level was calculated to lie about 4 kT below the center of the gap and was not significantly changed by radiation. Figure 8 is a plot of the forward current as a function of voltage for the median and the extremes before and after irradiation.

At moderate forward biases (from about 400 mV up to the built-in voltage of 0.77 V), the forward current is dominated by diffusion current (eq. (11)). The mean increase in diffusion current was approximately elevenfold. This is in fair agreement with the change in the square root of the base minority carrier lifetime τ_{n_0} (see table IV).

The radiation induced change in the lifetime is defined in terms of a damage constant K_τ , which is the change in the inverse lifetime per unit neutron fluence:

$$\frac{1}{\tau_R} = \frac{1}{\tau_0} + K_\tau \varphi \quad (14)$$

where τ_R is the effective lifetime after irradiation, τ_0 is the initial effective lifetime, and φ is the total neutron fluence. The damage constants were calculated for these diodes in terms of the effective lifetimes as defined in equation (13). The values are shown in table IV. There appears to be a difference in the damage constant due to operating mode, but data scatter makes interpretation uncertain. Bilinski, et al., (ref. 14) present a compilation of experimental damage constants for silicon which range from 4×10^{-8} to 4×10^{-6} ((sec)(neutron)/cm²)⁻¹.

SUMMARY OF RESULTS

Twenty-five voltage-regulator (Zener) diodes (S1N2985) were exposed to reactor radiation to a fast-neutron fluence of 8×10^{13} neutrons per square centimeter and a gamma ray dose of 6×10^7 carbon. The following results were obtained:

1. The effects of neutron-induced carrier removal were negligible at this dose level; that is, those electrical characteristics that are dependent on carrier concentration were not significantly affected.

- a. Junction capacitance was unchanged. The maximum increase in the Zener voltage at 100 milliamperes was less than 1 percent.

- b. The breakdown knees were slightly softened.

2. The forward voltage drop at high current levels increased, in general, and the amount of increase was affected by the electrical operating conditions during irradiation. These effects were not explainable by current theory.

3. The minority-carrier lifetimes were decreased: the mean electron lifetime by a factor of 37 and the mean hole lifetime by a factor of 3.

a. These lifetime decreases caused about a factor of 10 increase in the reverse-leakage current and the forward current at biases below 400 millivolts.

b. The decrease in the electron lifetime also produces the factor of 11 increase in the forward current at biases between 400 and 700 millivolts.

Lewis Research Center,
National Aeronautics and Space Administration,
Cleveland, Ohio, August 22, 1968,
120-27-04-35-22.

APPENDIX - SYMBOLS

A	junction area, cm^2	n_p	electron concentration in base, cm^{-3}
a	grade constant, cm^{-4}	q	electron charge, C
b	parameter determined by trap level, lifetime, and applied bias	V_A	applied voltage, V
C	junction capacitance, F	V_B	built-in voltage, V
C_0	junction capacitance at zero bias, F	V_{br}	breakdown voltage, V
D_n	electron diffusion constant, cm^2/sec	V_Z	Zener voltage, V
d	base region width, cm	ΔV_Z	voltage regulation, V
$E_T - E_i$	separation of trap level from center of gap, eV	W	depletion region width, cm
f(b)	function of b	W_0	depletion region width at zero bias, cm
I	current, A	Z_{zK}	Zener impedance at 1.0 mA, ohm
I_{R_1}	reverse current at 18.8 V and 25°C , μA	Z_{zT}	Zener impedance at I_{zT} , ohms
I_{R_2}	reverse current at 18.8 V and 250°C , μA	ϵ	dielectric permittivity of silicon, F/cm
I_{zM}	maximum Zener current, A	μ	minority carrier mobility, $\text{cm}^2/(\text{V})(\text{sec})$
I_{zS}	maximum surge current, A	τ_{n_0}	minority carrier lifetime in p-type material, sec
I_{zT}	Zener test current, mA	τ_0	preirradiation effective lifetime, sec
K_T	damage constant, $(\text{nvt})(\text{sec})^{-1}$	τ_{p_0}	minority carrier lifetime in n-type material, sec
kT	Boltzmann's constant times temperature, eV	τ_R	postirradiation effective lifetime, sec
L_n	electron diffusion length, cm	φ	fast neutron fluence, neutrons/ cm^2
N_B	doping density in base, cm^{-3}		
n_i	intrinsic carrier concentration, cm^{-3}		

REFERENCES

1. Been, Julian F.: Effects of Nuclear Radiation on a High-Reliability Silicon Power Diode. I - Change in I-V Design Characteristics. NASA TN D-4620, 1968.
2. Thatcher, R. K.; Hamman, D. J.; Chapin, W. E.; Hanks, C. L.; and Wyler, E. N.: The Effect of Nuclear Radiation on Electronic Components, Including Semiconductors. Rep. REIC 36, Battelle Memorial Inst., Oct. 1, 1964. (Available from DDC as AD-454707.)
3. Lockridge, R. W.: Screening Specification for Semiconductor Devices S1N2970B thru S1N2985B. Specification 85 M01307, NASA George C. Marshall Space Flight Center, Apr. 1963.
4. Smith, John R.; Kroeger, Erich W.; Asadourian, Arman S.; and Spagnuolo, Adolph C.: Fast-Neutron Beam Irradiation Facility in the NASA Plum Brook Test Reactor. NASA TM X-1374, 1967.
5. Bozek, John M.; and Godlewski, Michael P.: Experimental Determination of Neutron Fluxes in Plum Brook Reactor HB-6 Facility with Use of Sulfur Pellets and Gold Foils. NASA TM X-1497, 1968.
6. Bloomfield, Harvey S.: Calculation of Fast-Neutron Flux Emerging From a Reactor Beamhole and Comparison with Experiment. NASA TM X-1418, 1967.
7. Bozek, John M.: Experimental Determination of Gamma Exposure Rate in Plum Brook HB-6 Facility. NASA TM X-1490, 1968.
8. Stein, H. J.: Introduction Rate of Electrically Active Defects in n-Type Silicon by Nuclear Radiation. Rep. SC-DC-65-1274, Sandia Corp., June 25, 1965.
9. Moll, John L.: Physics of Semiconductors. McGraw-Hill Book Co., Inc., 1964.
10. Muss, D. R.: Capacitance Measurements on Alloyed Indium-Germanium Junction Diodes. J. Appl. Phys., vol. 26, no. 12, Dec. 1955, pp. 1514-1517.
11. Phillips, A. B.: Transistor Engineering: An Introduction to Integrated Semiconductor Circuits. McGraw-Hill Book Co., Inc., 1962.
12. Jonscher, A. K.: Principles of Semiconductor Device Operation. John Wiley & Sons, Inc., 1960.
13. Sah, Chik-Tarry; Noyce, Robert N.; and Shockley, William: Carrier Generation and Recombination of P-N Junctions and P-N Junction Characteristics. Proc. IRE, vol. 45, no. 9, Sept. 1957, pp. 1228-1243.
15. Bilinski, J. R.; Brooks, E. H.; Cocca, U.; and Maier, R. J.: Proton-Neutron Damage Equivalence in Si and Ge Semiconductors. IEEE Trans. on Nucl. Sci., vol. NS-10, no. 5, Nov. 1963, pp. 71-86.

FIRST CLASS MAIL

POSTMASTER: If Undeliverable (Section 158
Postal Manual) Do Not Return

"The aeronautical and space activities of the United States shall be conducted so as to contribute . . . to the expansion of human knowledge of phenomena in the atmosphere and space. The Administration shall provide for the widest practicable and appropriate dissemination of information concerning its activities and the results thereof."

— NATIONAL AERONAUTICS AND SPACE ACT OF 1958

NASA SCIENTIFIC AND TECHNICAL PUBLICATIONS

TECHNICAL REPORTS: Scientific and technical information considered important, complete, and a lasting contribution to existing knowledge.

TECHNICAL NOTES: Information less broad in scope but nevertheless of importance as a contribution to existing knowledge.

TECHNICAL MEMORANDUMS: Information receiving limited distribution because of preliminary data, security classification, or other reasons.

CONTRACTOR REPORTS: Scientific and technical information generated under a NASA contract or grant and considered an important contribution to existing knowledge.

TECHNICAL TRANSLATIONS: Information published in a foreign language considered to merit NASA distribution in English.

SPECIAL PUBLICATIONS: Information derived from or of value to NASA activities. Publications include conference proceedings, monographs, data compilations, handbooks, sourcebooks, and special bibliographies.

TECHNOLOGY UTILIZATION PUBLICATIONS: Information on technology used by NASA that may be of particular interest in commercial and other non-aerospace applications. Publications include Tech Briefs, Technology Utilization Reports and Notes, and Technology Surveys.

Details on the availability of these publications may be obtained from:

SCIENTIFIC AND TECHNICAL INFORMATION DIVISION
NATIONAL AERONAUTICS AND SPACE ADMINISTRATION
Washington, D.C. 20546